

Tropical forest leaves may darken in response to climate change

Christopher E. Doughty^{1*}, Paul Efren Santos-Andrade², Alexander Shenkin³, Gregory R. Goldsmith⁴, Lisa P. Bentley⁵, Benjamin Blonder³, Sandra Díaz⁶, Norma Salinas^{2,7}, Brian J. Enquist⁸, Roberta E. Martin⁹, Gregory P. Asner⁹ and Yadvinder Malhi³

Tropical forest leaf albedo (reflectance) greatly impacts how much energy the planet absorbs; however, little is known about how it might be impacted by climate change. Here, we measure leaf traits and leaf albedo at ten 1-ha plots along a 3,200-m elevation gradient in Peru. Leaf mass per area (LMA) decreased with warmer temperatures along the elevation gradient; the distribution of LMA was positively skewed at all sites indicating a shift in LMA towards a warmer climate and future reduced tropical LMA. Reduced LMA was significantly ($P < 0.0001$) correlated with reduced leaf near-infrared (NIR) albedo; community-weighted mean NIR albedo significantly ($P < 0.01$) decreased as temperature increased. A potential future 2 °C increase in tropical temperatures could reduce lowland tropical leaf LMA by 6–7 g m⁻² (5–6%) and reduce leaf NIR albedo by 0.0015–0.002 units. Reduced NIR albedo means that leaves are darker and absorb more of the Sun's energy. Climate simulations indicate this increased absorbed energy will warm tropical forests more at high CO₂ conditions with proportionately more energy going towards heating and less towards evapotranspiration and cloud formation.

Tropical forests are the most important terrestrial biome affecting planetary albedo through both surface effects and impacts on cloud cover, which in turn drive global climate¹. Humans have already increased the albedo of South American tropical forest regions through land use change, which has increased by 0.0025 albedo units across South America². However, little is known about how tropical forest leaf albedo could be affected by climate change. Tropical forest canopy albedo is principally a function of leaf albedo and leaf area index, with the latter typically high and saturated in terms of its contribution to albedo³. Leaf reflectance in the visible (VIS) portion of the solar-reflected spectrum (VIS, 400–700 nm) tends to be driven by leaf traits, such as chlorophyll content, while near-infrared (NIR) leaf reflectance (NIR, 700–2,500 nm) tends to be driven more by structural traits, such as leaf mass per area (LMA)^{4–7}.

Trait-based ecological scaling theory predicts that plant traits will change in response to increasing global temperatures and provides a basis for evaluating the potential effects on albedo. This theory posits that there is an optimal set of traits to maximize plant growth for any given environment^{8–11}. However, in a rapidly changing climate, the extant and optimal trait values may differ and be out of equilibrium. When this occurs, mean trait distributions can be skewed, as they are in the process of shifting towards the optimal trait distributions for the new climate. We recently demonstrated that the distributions of LMA and leaf percentage phosphorus concentration were positively skewed across a series of ten 1-ha plots along an elevation transect in Peru (Supplementary Table 1)^{9,12}. This suggested that they had begun their migration towards a new optimal distribution for a warmer world and were not yet in equilibrium. In other words, we expect leaf traits may change everywhere due to a changing climate,

but we expect to first see such trends along elevation gradients and within the trait distributions of existing plots. Along the same elevation transect, it has been demonstrated that the mean distribution of many tree genera have shifted upwards^{13,14}. However, such upward shifts were fewer than may have been expected based on the large temperature changes that had occurred in the region, a second indication suggesting that the trees are in a state of disequilibrium.

To measure whether traits will continue to shift in sensitive ecosystems, such as tropical montane systems, LMA has been suggested as a proxy for tracking forest response to climate change¹². This is because changes in LMA have been statistically correlated with changes to temperature, and increased temperatures along a Peruvian elevation gradient led to decreased LMA values⁹. This result was evident in both field results and at multiple spatial scales (0.1–1 ha resolution) using remote sensing¹². Several other tropical and temperate forest studies have shown similar LMA elevation trends, possibly because cooler and more adverse growing conditions lead to a more conservative plant resource strategy^{15–17}. Cold temperatures lead to reduced cell expansion, many small cells per unit area and, thus, more cell wall material per unit leaf volume and more cell layers¹⁸. More cell layers reduce freezing stress through slowing down the freezing rate¹⁹. LMA also decreases at higher temperatures, but not at the same rate as at lower temperatures²⁰.

Leaf structural traits, such as LMA, strongly influence leaf reflectance and transmittance, particularly in tropical forest foliage²¹. LMA is correlated with these structural parameters and (assuming cell walls have a constant weight per unit area) an increase in LMA will increase the cell wall interfaces in a leaf²². Leaf reflectance models, such as PROSPECT^{6,23,24}, simulate leaf reflectance using (among

¹School of Informatics, Computing, and Cyber Systems, Northern Arizona University, Flagstaff, AZ, USA. ²Universidad Nacional San Antonio Abad del Cusco, Cusco, Peru. ³Environmental Change Institute, School of Geography and the Environment, University of Oxford, Oxford, UK. ⁴Schmid College of Science and Technology, Chapman University, Orange, CA, USA. ⁵Department of Biology, Sonoma State University, Rohnert Park, CA, USA. ⁶Instituto Multidisciplinario de Biología Vegetal, CONICET and Universidad Nacional de Córdoba, Córdoba, Argentina. ⁷Sección Química, Pontificia Universidad Católica del Perú, Lima, Peru. ⁸Department of Ecology and Evolutionary Biology, University of Arizona, Tucson, AZ, USA. ⁹Department of Global Ecology, Carnegie Institution for Science, Stanford, CA, USA. *e-mail: chris.doughty@nau.edu

other factors) structural trait-based parameters that relate to the cellular arrangement of the leaf. For instance, in PROSPECT, a plant leaf is modelled as a series of leaf layers with a refractive index and an absorption coefficient. An example of a leaf with a low structure value would be a leaf with a compact mesophyll, and an example of a leaf with a high structure value would be a leaf with spongy parenchyma and lower cell density. LMA is tightly correlated with the structure term^{6,25}. We use the PROSPECT model to predict changes to leaf albedo in response to a change in LMA^{6,24}.

Measured leaf reflectance can be averaged to derive leaf albedo, which can be fed into climate models to better constrain surface albedo. Vegetation models embedded within climate models, such as the National Center for Atmospheric Research (NCAR)'s Community Earth System Model can be used to study how changes in tropical leaf albedo may impact global climate²⁶. Canopy albedo in many land surface models is driven by VIS and NIR leaf albedo embedded in a two-stream canopy radiative transfer model²⁷. Planetary albedo, another calculated albedo parameter, integrates canopy albedo and atmosphere albedo, which mainly varies due to changes in percentage cloud cover. Changes to leaf albedo will impact both planetary albedo and surface albedo because albedo-driven thermal changes to leaves will impact latent heat fluxes and cloud cover. A decrease in leaf albedo can either increase sensible heat fluxes (and leaf temperature) or increase latent heat fluxes (and leaf transpiration). How a leaf partitions this energy following a leaf albedo change may vary with latitude²⁸. For instance, increasing leaf albedo by 0.15 albedo units in climate simulations had a greater impact at high (>30°) than at low latitudes (<30°) (a 0.08 versus 0.06 increase in surface albedo, respectively). At low latitudes, models estimate that a reduction in leaf albedo tends to increase latent heat fluxes, while a reduction in leaf albedo in high-latitude areas tends to increase sensible heat fluxes. This increase in latent heat fluxes at low latitudes increases cloud formation, thereby forming a partial offset to land surface albedo changes²⁸. How energy is partitioned following a change in leaf albedo has major potential implications on global climate.

In the current study, we assess the relationship between tropical forest LMA and leaf albedo (VIS, 400–700 nm and NIR, 701–1,075 nm) by measuring these traits on more than 4,000 leaves along a 3,200 m tropical forest elevation transect in Peru. We use trends in trait distributions, correlations between LMA and leaf albedo and a leaf reflectance model (PROSPECT) to predict future trends in LMA and leaf albedo in a scenario where the tropics are 2°C warmer than today (RCP4.5 scenario²⁹). We then use climate simulations (NCAR's Community Earth System Model) to predict how such changes in tropical leaf albedo could impact both regional and global climate under variable atmospheric CO₂ concentrations (367 and 700 ppm).

Results

Leaf LMA was highly significantly correlated ($P < 0.0001$) (Fig. 1) with both NIR and VIS leaf albedo. Previous research using this data set found that LMA is linearly related to elevation and that temperature is the driving factor⁹. Skewness in the distribution will probably not affect these trends since skewness is relatively consistent across plots (Supplementary Table 1). LMA is related to temperature in both field ($-3.6 \text{ g m}^{-2} \text{ per } ^\circ\text{C}$) and remote sensing ($-3.0 \text{ g m}^{-2} \text{ per } ^\circ\text{C}$) data¹². With a hypothetical 2°C change in future temperatures²⁹, we might expect a future decrease in LMA between 6 and 7 g m^{-2} (a 5–6% change based on the mean sunlit leaf LMA of $109 \pm 44 \text{ g m}^{-2}$). According to the relationship between LMA and leaf NIR albedo (Fig. 1), we might predict a decrease in NIR albedo of 0.0015–0.002 albedo units with a 2°C warming.

There was no trend in visible-wavelength albedo (Fig. 2a), but basal area-weighted NIR leaf albedo decreased significantly ($P < 0.01$) (Fig. 2b) with increasing temperature with a slope of

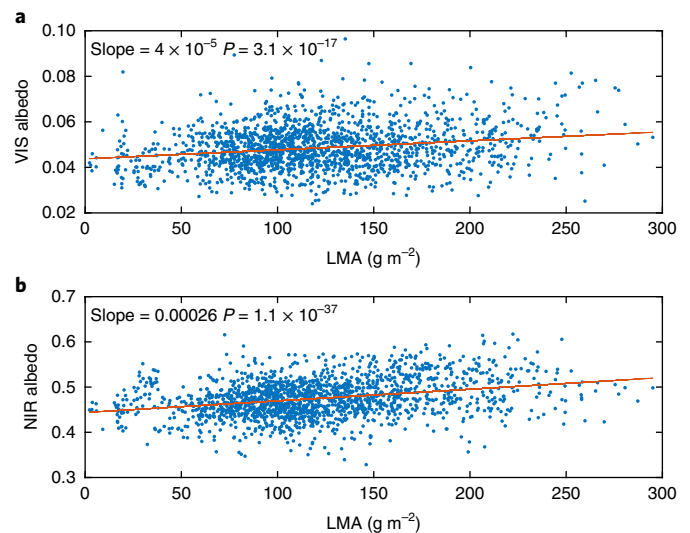


Fig. 1 Individual leaf albedo versus LMA. | **a, b**, Correlation between VIS (**a**; 400–700 nm) or NIR (**b**; 701–1,075 nm) leaf albedo and LMA (g m^{-2}) for all individual leaf measurements from a Peruvian elevation transect ($n = 1,733$).

-0.00065 albedo units per $^\circ\text{C}$. A previous study using this same leaf reflectance data set³⁰ found no trend in leaf albedo with elevation, but the data were not basal area-weighted. This suggests that dominant species show a stronger trend in albedo than rarer species in the NIR (but see Asner et al. 2017¹²). NIR albedo decreased by about 0.01 albedo units across the 15°C temperature gradient. If our trend in temperatures is reflective of future changes in a warmer world, then we might expect that with a 2°C increase in temperature²⁹ tropical forest NIR albedo could decrease by 0.0013 albedo units. This is similar in magnitude to an independent prediction of a direct comparison of community-weighted mean NIR leaf albedo to temperature (Fig. 1) (0.0015–0.002 albedo units).

We used the leaf reflectance model PROSPECT v4 with basal area-weighted mean plot-measured values ($n = 9$) for chlorophyll ($\mu\text{g cm}^{-2}$), water (g cm^{-2}) and dry matter (g cm^{-2}) (Supplementary Table 2), and converted LMA values to N structure layers following equation (1) and found a slope of -0.0015 NIR albedo units per $^\circ\text{C}$ (Fig. 2c). To understand the impact of other trait changes on leaf albedo, we then ran the model with constant chlorophyll, percentage water and carbon but changing LMA and found a slope of -0.0017 albedo unit per $^\circ\text{C}$. With a predicted 2°C increase in temperature, we predict a decrease in NIR leaf albedo of 0.0030–0.0034 or approximately double our predicted change based on measurements (Fig. 2b).

For a location in the Western Amazon close to our field sites (latitude -13 , longitude -69), at current CO₂ concentrations (367 ppm) the coupled land and atmosphere model predicts that a decrease in leaf NIR albedo leads to a linear increase (slope 15 W m^{-2} per unit NIR albedo) in latent heat flux, but little change in sensible heat fluxes (Fig. 3a,b and Table 1). However, at 700 ppm CO₂ concentrations the model predicts a more even distribution (7 latent heat versus 4 sensible heat W m^{-2} per unit albedo) between sensible and latent heat fluxes (Fig. 3a,b and Table 1). This difference in energy partitioning had large additional climate impacts. For instance, at current CO₂ concentrations, these increases in latent heat fluxes increase cloud cover (Fig. 3c) and rainfall (Fig. 3d) linearly (slopes 0.07% cloud cover per unit albedo and $3.5 \times 10^5 \text{ mm s}^{-1}$ per unit albedo, respectively). At current CO₂ concentrations, leaf temperature (Fig. 3e) does not change since there is little change in sensible heat fluxes; however, at high CO₂ concentrations leaves warm by 0.23 K unit albedo⁻¹. Photosynthesis increases linearly (Fig. 3g)

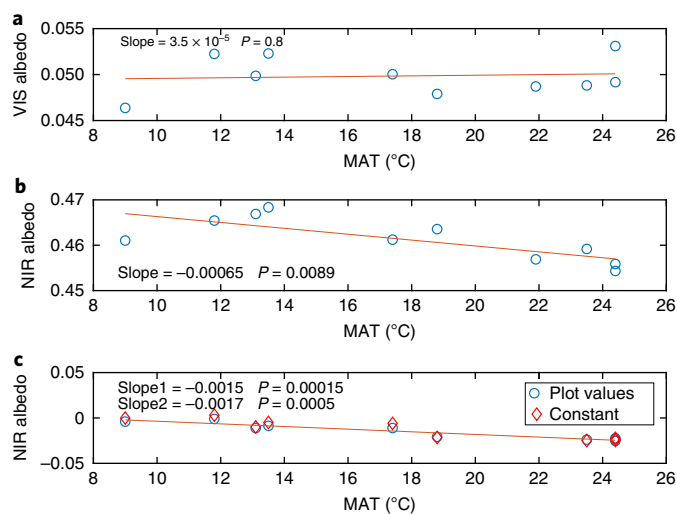


Fig. 2 | Basal area-weighted plot averaged albedo. a, VIS leaf albedo (400–700 nm) versus plot mean annual temperature (MAT) from 10 1-ha plots. **b**, NIR leaf albedo (701–1,075 nm) versus plot MAT from 10 1-ha plots. **c**, Change in NIR albedo using PROSPECT parameterized with plot-specific basal area-weighted LMA, percentage water, chlorophyll content and percentage dry matter (blue), keeping all parameters constant except for LMA (red).

(slope $-0.55 \mu\text{mol m}^{-2} \text{s}^{-1}$ per unit albedo) with leaf albedo. The impact of decreased leaf albedo has \sim twice the impact on planetary albedo at 700 ppm versus 367 ppm (4.6 versus 2.9 W m^{-2} per unit albedo) (Fig. 3h) because cloud cover increases as leaf albedo decreases (Fig. 3c). Generally, at high CO_2 concentrations there was less increase in cloud cover and rainfall, but greater increases in leaf and air temperatures.

Our spatial map (Fig. 4) shows that most tropical regions showed similar trends to the pixel described earlier. However, at both current and high CO_2 concentrations, the Eastern Amazon actually had increased cloud cover (Fig. 4f) and rainfall (Fig. 4d) with decreased leaf NIR albedo, a trend probably tied to the movement of the Inter Tropical Convergence Zone (ITCZ) and broad planetary energy balance^{31,32}. Likewise, while the tropics tends to reduce cloud cover, most temperate regions showed a reversed trend, a trend again reversed in boreal regions (Fig. 4). Most of the planetary-scale warming occurred in the tropics and again at high latitudes ($>60^\circ$ latitude) with little warming of temperate regions between 30 and 60° (Supplementary Figs. 2 and 4c). Given the linearity in many of the climate simulation trends (Fig. 3), we feel confident in applying them to the small predicted change in leaf albedo. Air temperatures for the terrestrial pantropics increased at twice the rate per unit albedo change at high atmospheric CO_2 concentrations (700 ppm) versus current CO_2 concentrations (367 ppm) (Fig. 3f, slope 0.23 versus 0.14°C per unit albedo, Supplementary Fig. 2) because proportionately more energy went towards sensible heat fluxes and less went towards latent heat fluxes. The reduction in latent heat fluxes also reduced cloud formation and allowed a larger change in planetary albedo. We estimate that this reduced tropical leaf albedo will warm the tropics between 0.0002 and 0.0005°C (Fig. 3f), or the equivalent of all CO_2 emissions from a major industrial country such as India or Japan for an entire year (see Methods for calculations).

Discussion

In a warmer future, lowland tropical tree species have three potential options: (1) those at their thermal maxima may die; (2) they may migrate upslope if they are located near mountains; or (3) they may

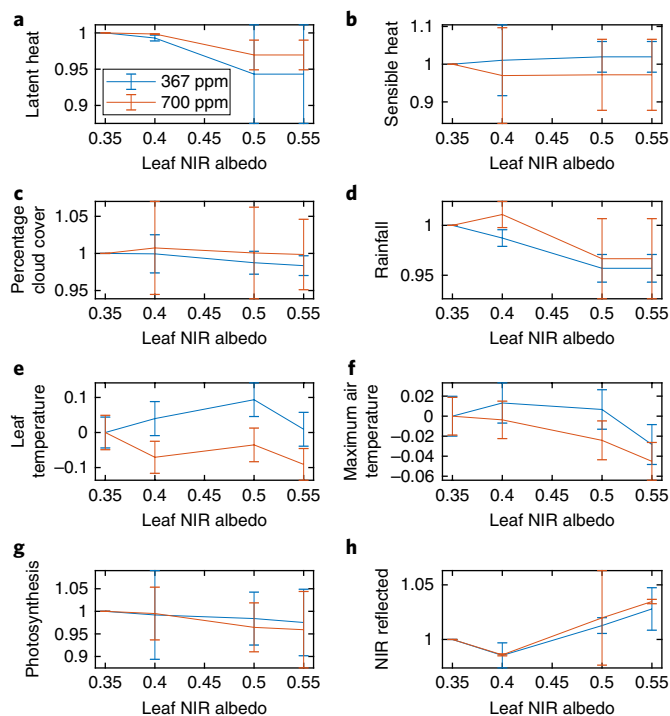


Fig. 3 | Four simulations averaging the last 50 years of a 100-year

simulation. Broadleaved evergreen tropical plant functional type leaf NIR albedo is 0.35, 0.40, 0.50 and 0.55, using the CLM 4.0 coupled with CAM 4.0 for a location in the Western Amazon approximately near our field sites (latitude -13 , longitude -69) with atmospheric CO_2 concentrations at 367 ppm (blue) and 700 ppm (red). **a**, Fractional changes from 0.35 albedo runs for latent heat fluxes. **b**, Fractional changes from 0.35 albedo runs for sensible heat fluxes (W m^{-2}). **c**, Fractional changes from 0.35 albedo runs for percentage cloud cover. **d**, Fractional changes from 0.35 albedo runs for rainfall (mm month^{-1}). **e**, Fractional changes from 0.35 albedo runs for absolute change in leaf temperature. **f**, Fractional changes from 0.35 albedo runs for maximum daily 2 m air temperature (K) across the terrestrial tropics. **g**, Fractional changes from 0.35 albedo runs for photosynthesis ($\mu\text{mol m}^{-2} \text{s}^{-1}$). **h**, Fractional changes from 0.35 albedo runs for direct reflected NIR planetary albedo (W m^{-2}). Data represent mean ± 1 s.e.m.

shift their traits to better acclimate to warmer conditions. All three may already be occurring. For instance, tropical tree mortality may be increasing, possibly in response to climate change³³. Tree species may be shifting up the elevation transect¹⁴. Finally, significant skewness of traits can indicate that the traits within the community are potentially shifting in response to shifts in climate⁹. Our lowland sites (Tambopata 5 and 6, ~ 200 m elevation) have strong positive skewness of LMA from both field⁹ and remotely sensed data¹², which may be indicative of shifts in LMA within the broader tropics (Supplementary Table 1).

Changes in LMA are generally coupled to changes in other traits, including percentage nitrogen and photosynthetic capacity, as described in the leaf economics spectrum³⁴. Other lowland leaf traits also showed strong positive skewness, including percentage phosphorous, percentage nitrogen and photosynthetic capacity. However, other studies demonstrate that leaf phosphorous is skewed within a site due to microsite variability³⁵. It is unclear whether the predicted decrease in LMA in the lowland tropics will also impact percentage phosphorous and photosynthetic capacity, which are more correlated to local nutrient limitations³⁶. Recent work shows that a decrease in LMA is correlated with reduced cell wall mass per leaf area, younger leaves and decreased mesophyll

Table 1 | Results of climate simulations in which we changed tropical leaf NIR albedo at 367 ppm and 700 ppm

	Latent heat (W m ⁻²)	Sensible heat (W m ⁻²)	Cloudy (%)	Rainfall (mm s ⁻¹)	Leaf temperature (K)	Photosynthesis (μmol m ⁻² s ⁻¹)	Planetary albedo (W m ⁻²)
Slope (variable/ change in NIR tropical leaf albedo)	-14.9/ -6.77	2.6/ -4.2	-0.07/ 0.003	-0.00003/ -0.00002	0.05/ -0.45	-0.73/ -2.1	2.9/ 4.6
Mean variable value	38.16/ 32.9	20.13/ 21.7	0.785/ 0.80	0.00011/ 0.00012	298.9/ 299.3	6.81/ 8.8	35.08/ 35.4
Percentage change with a 0.0015 and 0.0034 decrease in NIR leaf albedo	0.06-0.13/ 0.03-0.07	-0.02 to -0.04/ 0.029-0.065	0.01-0.03/ -0.0006 to -0.001	0.04-0.10/ 0.03-0.07	-0.00002-0.00005/ -0.0002-0.0005	0.02-0.04/ 0.04-0.08	-0.01 to -0.03/ -0.02 to -0.04

Change in latent heat, sensible heat, cloud cover, rainfall, leaf temperature, photosynthesis and planetary albedo with a change (0.35–0.5) in leaf NIR albedo using NCAR's CLM 4.0 coupled to CAM-4.0 for a location in the Western Amazon approximately near our field sites (latitude -13, longitude -69). We show the slope (variable/0.015 change in NIR tropical leaf albedo), mean value at standard leaf NIR albedo (0.45) and predicted change based on the slope, and the predicted change in leaf NIR albedo (0.0015 and 0.0034 albedo units). Values are shown for 367 ppm (left) and 700 ppm (right, indicated in bold).

conductance³⁷. Reduced LMA will reduce the proportional allocation of carbon and nitrogen to cell walls and towards the photosynthetic machinery, which will also reduce diffusive limitations such as mesophyll conductance³⁸. This shift could theoretically increase photosynthetic capacity as leaves shift towards a 'live fast' strategy. Younger leaves can impact both LMA and leaf spectral properties³⁹. However, there was no trend in either leaf photosynthetic capacity⁹ or in chlorophyll content¹² along the gradient. Therefore, further research is necessary to understand the impact of changing LMA on other traits (and the potential leaf albedo impacts of such changes).

Both theory⁶ and field results (Figs. 1 and 2) indicate that a reduction in LMA will reduce tropical forest NIR leaf albedo. The PROSPECT model predicts a slightly larger change in NIR albedo when we parameterized leaf reflectance based on plot-specific values (0.003 versus 0.0015). This amount increases slightly (by 0.0004) when we fix other variables (chlorophyll, water and dry matter) at a constant value indicating that other traits along the gradient may slightly buffer the impact of changing LMA on albedo. We used changes over a spatial gradient (our elevation transect) to predict future changes in trait distributions—a space-for-time substitution method. However, although irreplaceable, such methods can introduce uncertainties⁴⁰; some of the differences between model and field results could be a result of this.

It is estimated that the tropics have warmed by 0.26 ± 0.05 °C per decade since the 1970s⁴¹. Although future temperature trends in the tropics are highly uncertain, most models estimate that under the RCP4.5 scenario, which stabilizes radiative forcing at 4.5 W m^{-2} in the year 2100, tropical forest temperature will increase by $1.5\text{--}2$ °C²⁹. Coupled Model Intercomparison Project Phase 5 predictions show regional distinctions with a wetter Western Amazon and drier Eastern Amazon⁴². Based on our empirical results, we hypothesize that such a trend in tropical temperatures would decrease LMA by $6\text{--}7 \text{ g m}^{-2}$, with a predicted reduction of leaf NIR albedo of between 0.0015 and 0.002 units. Atmospheric CO₂ concentrations and precipitation will also change. We do not know the impacts of these changes on LMA, but increased atmospheric CO₂ concentrations may increase VIS tropical leaf reflectance⁴³. There is also great uncertainty regarding future tropical temperatures, since this is primarily a function of anthropogenic greenhouse gas inputs.

Our model simulations suggest that, at current CO₂ concentrations, reduced leaf albedo will increase latent heat fluxes and transpiration leading to relatively stable leaf temperatures^{44,45}. This potential reduction of water use efficiency contrasts with predicted⁴⁶ and measured, in tropical tree rings⁴⁷, increases in water use efficiency due to CO₂ fertilization. However, under high CO₂ conditions the model estimates a more evenly distributed change in sensible and latent heat fluxes. It is difficult to have confidence in model-driven sensible/latent heat fluxes for the tropics because current models do not accurately capture tropical leaf temperatures that can reach temperatures

above 40 °C⁴⁸. For instance, our simulations did not predict that vegetation temperatures would generally exceed air temperatures, but empirical studies have shown that sunlit leaf temperatures generally exceed air temperatures by an average of 2–3 °C in the tropics⁴⁸. Rapidly changing sun shade conditions in tropical forests due to quickly changing cloud cover could inhibit the ability of stomata to equilibrate and maintain a steady leaf temperature. For instance, in an Amazonian tropical forest over 60% of direct photosynthetically active radiation during the dry season arrives in intervals with <10-min duration⁴⁸. If the models are incorrect and, due to the rapidly changing leaf microclimate of tropical forests, stomata cannot adjust and sensible heat fluxes (and leaf temperature) increase instead of latent heat fluxes (and transpiration), then a decrease in tropical leaf albedo could have drastically different results than predicted by model results at current CO₂ concentrations. For instance, increasing leaf temperatures could instead reduce total carbon uptake, as is currently seen during warm periods^{48,49}. Recent coupled earth system model simulations have shown that with climate change, decreased transpiration and increased sensible heat can reduce global photosynthesis by $2.7 \pm 1.76\%$ ⁵⁰. Therefore, a key future issue is to better understand empirically how a decrease in leaf albedo could impact the leaf-level latent-sensible heat ratio.

Our trait data from the Peruvian elevation transect indicate that decreased lowland LMA could reduce tropical NIR leaf albedo. Reduced NIR albedo means that the leaves are darker and will absorb more of the Sun's energy. Climate simulations indicate that darker leaves could lead to an increase in pantropical temperatures (Fig. 3f) that are exacerbated under high CO₂ scenarios. As CO₂ concentrations increase, more of the energy absorbed by tropical forest leaves will go towards heating instead of evapotranspiration and cloud formation. Therefore, increased CO₂ concentrations may reduce the negative feedback of reduced tropical leaf NIR albedo being cancelled out by increased atmosphere albedo (through increased cloud cover). More broadly, changes to South American albedo could impact the planet's surface energy balance, resulting in changes in the position of the ITCZ and global climate impacts^{31,32}, although the darkening of leaves predicted by this study may be too small to impact the ITCZ since it is not known if this process is linear. Leaves globally will experience similar pressures from climate change; the impact on leaf albedo would be much greater if leaf LMA and albedo changed globally, but further research is necessary to determine if leaf albedo may also change outside the tropics. Changing tropical leaf traits in response to climate change may be adaptable at the individual level, but it appears to exacerbate negative climate trends at the global scale.

Methods

Field sites. We measured leaf traits and albedo during the CHAMBASA (Challenging Attempt to Measure Biotic Attributes along the Slopes of the Andes)

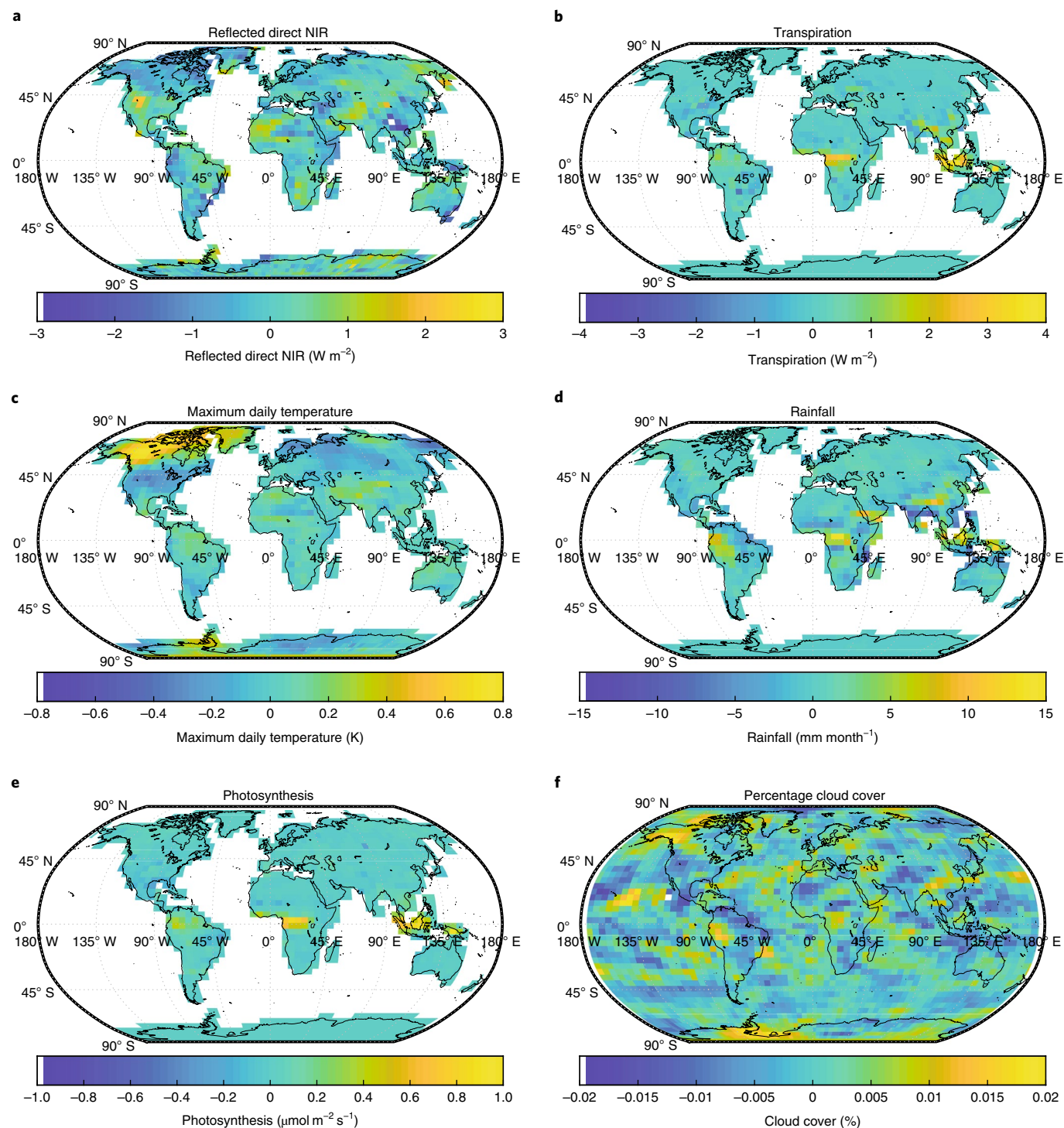


Fig. 4 Climate simulations with reduced tropical leaf NIR albedo. | Simulations of CLM 4.0 coupled with CAM-4.0 for 100 years averaging over the last 50 years, for which we reduced tropical NIR leaf albedo by 0.2 (subtracting a run at 0.35 from a run at 0.55) at 700 ppm atmospheric CO_2 concentrations. **a**, Change in direct reflected NIR surface albedo (W m^{-2}). **b**, Change in latent heat fluxes (W m^{-2}). **c**, Change in maximum daily 2 m air temperature (K). **d**, Change in precipitation (mm month^{-1}). **e**, Change in photosynthesis ($\mu\text{mol m}^{-2} \text{s}^{-1}$). **f**, Change in percentage cloud cover. Significant pixels are shown in Supplementary Fig. 3.

campaign⁵¹ from April to November 2013 along an elevation transect (from 3,500 to 220 m above sea level; Supplementary Table 1) in the Peruvian Amazon⁵². The plots are part of a long-term research effort coordinated by the Andes Biodiversity Ecosystems Research Group (ABERG, <http://www.andesconservation.org>) and are part of the ForestPlots (<https://www.forestplots.net/>) and GEM networks (<http://gem.tropicalforests.ox.ac.uk/projects/aberg>). Plots were established between 2003 and 2013 in areas with minimal evidence of human disturbance. Within each

plot, all stems ≥ 10 cm in diameter at breast height were tagged and identified to species level. There is a negative linear relationship in the gradient between mean annual temperature (MAT) and elevation, with a MAT of 24.4°C in the warmest lowland Amazonian site and 9.0°C at the Amazonian treeline in the Andes. Mean annual precipitation varies from 1,560 to 5,302 mm y^{-1} along the elevation gradient. Soils at elevations > 600 m above sea level are comprised of relatively high-fertility inceptisols and entisols. Soils at elevations < 600 m above sea level vary among

ultisols on low-fertility terra firma clay substrates and inceptisols on inactive high-fertility floodplains. Plot characteristics are shown in Supplementary Table 1.

Leaf collection sampling strategy. In each 1-ha plot ($n = 10$ plots), we sampled the most abundant species as determined through basal area weighting (enough species to account for 80% of the plot's basal area, although in the diverse lowland plots only 60–70% of plot basal area was sampled). For each species, we sampled the five (three in the lowlands) largest trees (based on diameter at breast height); tree climbers with extended tree pruners removed one fully sunlit and one shaded branch. These branches were quickly recut underwater to restore hydraulic conductivity. On each of these branches, we measured five randomly chosen leaves for photosynthesis and leaf spectral properties (generally measured within 1 h of being cut). The LMA for these leaves was measured on the same day.

Leaf spectroscopy. Hemispherical reflectance was measured on the top and bottom surface of five randomly selected leaves. The spectral measurements were taken at, or close to, the midpoint between the main vein and the leaf edge, and approximately halfway from the petiole to the leaf tip. Care was taken to avoid large primary or secondary veins, while allowing for smaller veins to be incorporated in the measurement. The spectra were collected with a Fieldspec Handheld 2 (Analytical Spectral Devices); this has a fibre optic cable contact probe that has its own calibrated light source and a leaf clip (High Intensity Contact Probe and Leaf Clip). The spectrometer records 750 bands spanning the 325–1075 nm wavelength range. Measurements were collected with a 136-ms integration time per spectrum. We optimized the spectrometer after every branch. We calibrated the spectrometer on every leaf for dark current and stray light, and white-referenced the measurement to a calibration panel (Spectralon; Labsphere). We averaged 25 individual spectra per leaf to improve the signal-to-noise ratio of the data. We compared leaf albedo to LMA using a linear regression model.

Climate simulation. We ran simulations using NCAR's Community Atmosphere Model (CAM-4.0; <http://www.cesm.ucar.edu/models/ccsm4.0/cam/>), coupled with the Community Land Model (CLM 4.0; <http://www.cgd.ucar.edu/tss/clm/>) with prescribed surface ocean temperatures⁵³, a river transport model and the Los Alamos Sea Ice Model. Simulations were run at a 20-min time step with a resolution of 2° by 2.5° at the equator for 100 years. We specifically ran the model using compset F_2000_CN, which uses the models described above. We ran the model with no dynamic vegetation response; atmospheric CO₂ was held constant at 367 ppm for one set of runs and 700 ppm for the other set. Prescribed surface ocean temperatures were modern for both CO₂ scenarios. We simulated global climate for scenarios where NIR leaf-level reflectance for the tropical evergreen broadleaved plant functional type was increased by 0.05 and 0.10, and decreased by 0.05 and 0.10 (control = 0.45). These large changes to leaf albedo were chosen to clearly demonstrate a change. If the relationships were found to be linear, we would scale the global climate predictions by our estimated changes in leaf albedo. The canopy albedo in CLM was calculated using a two-stream radiation transfer model, which is a function of leaf and stem area index, leaf albedo and transmittance, and the cosine of the zenith angle of the incident beam radiation, among other parameters⁵⁷. Significant differences were determined using a two-tailed *t*-test for the last 50 years.

We averaged the final 50 years of the following variables (collected monthly) from CLM 4.0: surface albedo ($W m^{-2}$); latent heat flux ($W m^{-2}$); sensible heat flux ($W m^{-2}$); vegetation temperature (K); photosynthesis ($\mu mol m^{-2} s^{-1}$); rainfall ($mm s^{-1}$); and cloud cover (%) from CAM-4.0.

We used a very simplistic method to demonstrate the equivalent of the albedo effect in terms of CO₂ emissions. Let us assume that global temperatures have increased by 0.8 °C with a CO₂ increase from 280 to ~400 ppm⁵⁴. Therefore, a 1 ppm increase is approximately equal to a global temperature increase of 0.0067 °C. Our estimates for increased tropical temperatures due to the albedo decrease are 0.0002–0.0005 °C or equivalent to between 0.03 and 0.07 ppm atmospheric CO₂ increase. Long-term average increases of CO₂ concentrations are ~1 ppm⁵⁵. Therefore, the impact of this effect for the tropics could be approximately equivalent to the CO₂ emissions of India (7%) or Japan (3%)⁵⁵ over a year.

PROSPECT model. To predict theoretical leaf reflectance, we used PROSPECT v4 (<http://teledetection.ipgp.jussieu.fr/prosail/>). We parameterized the model using measured basal area-weighted plot-level values of chlorophyll ($\mu g cm^{-2}$), water ($g cm^{-2}$) and dry matter ($g cm^{-2}$) (Supplementary Table 2)¹². We converted basal area-weighted plot LMA to the structure parameter *N* following Ceccato et al. (2001)³⁵ shown as equation (1). Based on PROSPECT, we calculated the basal area-weighted leaf reflectance for each plot. We also calculated reflectance assuming chlorophyll, percentage dry matter and percentage water were constant but LMA varied.

$$N = 4 \sqrt{\left(\frac{1}{LMA - 0.1} \right)} \quad (1)$$

Reporting Summary. Further information on research design is available in the Nature Research Reporting Summary linked to this article.

Data availability

All the data in this paper can be found in a data repository at the following website: <https://ora.ox.ac.uk/objects/uuid:4101e249-3cf5-443f-9c29-9204604c667b>.

Received: 17 April 2018; Accepted: 10 October 2018;

Published online: 19 November 2018

References

- Betts, R. Implications of land ecosystem-atmosphere interactions for strategies for climate change adaptation and mitigation. *Tellus B* **59**, 602–615 (2007).
- Loarie, S. R., Lobell, D. B., Asner, G. P. & Field, C. B. Land-cover and surface water change drive large albedo increases in South America. *Earth Interact.* **15**, 1–16 (2011).
- Asner, G. P. Biophysical and biochemical sources of variability in canopy reflectance. *Remote Sens. Environ.* **64**, 234–253 (1998).
- Serbin, S. P., Singh, A., McNeil, B. E., Kingdon, C. C. & Townsend, P. A. Spectroscopic determination of leaf morphological and biochemical traits for northern temperate and boreal tree species. *Ecol. Appl.* **24**, 1651–1669 (2014).
- Richardson, A. D., Duigan, S. P. & Berlyn, G. P. An evaluation of noninvasive methods to estimate foliar chlorophyll content. *New Phytol.* **153**, 185–194 (2002).
- Jacquemoud, S. & Baret, F. PROSPECT: a model of leaf optical properties spectra. *Remote Sens. Environ.* **34**, 75–91 (1990).
- Asner, G. P. & Martin, R. E. Spectral and chemical analysis of tropical forests: scaling from leaf to canopy levels. *Remote Sens. Environ.* **112**, 3958–3970 (2008).
- Enquist, B. J. et al. Scaling from traits to ecosystems: developing a general trait driver theory via integrating trait-based and metabolic scaling theories. *Adv. Ecol. Res.* **52**, 249–318 (2015).
- Enquist, B. J. et al. Assessing trait-based scaling theory in tropical forests spanning a broad temperature gradient. *Glob. Ecol. Biogeogr.* **26**, 1357–1373 (2017).
- Savage, V. M., Webb, C. T. & Norberg, J. A general multi-trait-based framework for studying the effects of biodiversity on ecosystem functioning. *J. Theor. Biol.* **247**, 213–229 (2007).
- Norberg, J. et al. Phenotypic diversity and ecosystem functioning in changing environments: a theoretical framework. *Proc. Natl Acad. Sci. USA* **98**, 11376–11381 (2001).
- Asner, G. P. et al. Scale dependence of canopy trait distributions along a tropical forest elevation gradient. *New Phytol.* **214**, 973–988 (2017).
- Feeley, K. J. et al. Upslope migration of Andean trees. *J. Biogeogr.* **38**, 783–791 (2011).
- Feeley, K. J. Distributional migrations, expansions, and contractions of tropical plant species as revealed in dated herbarium records. *Glob. Chang. Biol.* **18**, 1335–1341 (2012).
- Asner, G. P. & Martin, R. E. Convergent elevation trends in canopy chemical traits of tropical forests. *Glob. Chang. Biol.* **22**, 2216–2227 (2016).
- Körner, C. H., Bannister, P. & Mark, A. F. Altitudinal variation in stomatal conductance, nitrogen content and leaf anatomy in different plant life forms in New Zealand. *Oecologia* **69**, 577–588 (1986).
- Roderick, M. L., Berry, S. L. & Noble, I. R. A framework for understanding the relationship between environment and vegetation based on the surface area to volume ratio of leaves. *Funct. Ecol.* **14**, 423–437 (2000).
- Atkin, O. K., Loveys, B. R., Atkinson, L. J. & Pons, T. L. Phenotypic plasticity and growth temperature: understanding interspecific variability. *J. Exp. Bot.* **57**, 267–281 (2006).
- Ball, M. C. et al. Space and time dependence of temperature and freezing in evergreen leaves. *Funct. Plant Biol.* **29**, 1259–1272 (2002).
- Poorter, H., Niinemets, Ü., Poorter, L., Wright, I. J. & Villar, R. Causes and consequences of variation in leaf mass per area (LMA): a meta-analysis. *New Phytol.* **182**, 565–588 (2009).
- Asner, G. P. et al. Taxonomy and remote sensing of leaf mass per area (LMA) in humid tropical forests. *Ecol. Appl.* **21**, 85–98 (2011).
- Niinemets, Ü. Research review. Components of leaf dry mass per area—thickness and density—alter leaf photosynthetic capacity in reverse directions in woody plants. *New Phytol.* **144**, 35–47 (1999).
- Féret, J.-B. et al. PROSPECT-4 and 5: advances in the leaf optical properties model separating photosynthetic pigments. *Remote Sens. Environ.* **112**, 3030–3043 (2008).
- Féret, J.-B., Gitelson, A. A., Noble, S. D. & Jacquemoud, S. PROSPECT-D: towards modeling leaf optical properties through a complete lifecycle. *Remote Sens. Environ.* **193**, 204–215 (2017).
- Ceccato, P., Flasse, S., Tarantola, S., Jacquemoud, S. & Grégoire, J.-M. Detecting vegetation leaf water content using reflectance in the optical domain. *Remote Sens. Environ.* **77**, 22–33 (2001).

26. Collins, W. D. et al. The Community Climate System Model version 3 (CCSM3). *J. Clim.* **19**, 2122–2143 (2006).
27. Dickinson, R. E., Sellers, P. J. & Kimes, D. S. Albedos of homogeneous semi-infinite canopies: comparison of two-stream analytic and numerical solutions. *J. Geophys. Res. Atmos.* **92**, 4282–4286 (1987).
28. Doughty, C. E., Field, C. B. & McMillan, A. M. S. Can crop albedo be increased through the modification of leaf trichomes, and could this cool regional climate? *Clim. Change* **104**, 379–387 (2011).
29. Collins, M. et al. *Climate Change 2013: The Physical Science Basis* (eds Stocker, T. F. et al.) Ch. 29 (IPCC, Cambridge Univ. Press, 2013).
30. Doughty, C. E. et al. Can leaf spectroscopy predict leaf and forest traits along a Peruvian tropical forest elevation gradient? *J. Geophys. Res. Biogeosci.* **122**, 2952–2965 (2017).
31. Swann, A. L. S., Fung, I. Y. & Chiang, J. C. H. Mid-latitude afforestation shifts general circulation and tropical precipitation. *Proc. Natl Acad. Sci. USA* **109**, 712–716 (2012).
32. Doughty, C. E., Loarie, S. R. & Field, C. B. Theoretical impact of changing albedo on precipitation at the southernmost boundary of the ITCZ in South America. *Earth Interact.* **16**, 1–14 (2012).
33. Brienen, R. J. W. et al. Long-term decline of the Amazon carbon sink. *Nature* **519**, 344–348 (2015).
34. Wright, I. J. et al. The worldwide leaf economics spectrum. *Nature* **428**, 821–827 (2004).
35. Chadwick, D. K. & Asner, G. P. Organismic-scale remote sensing of canopy foliar traits in lowland tropical forests. *Remote Sens.* **8**, 87 (2016).
36. Fyllas, N. M. et al. Basin-wide variations in foliar properties of Amazonian forest: phylogeny, soils and climate. *Biogeosciences* **6**, 2677–2708 (2009).
37. Reich, P. B. & Flores-Moreno, H. Peeking beneath the hood of the leaf economics spectrum. *New Phytol.* **214**, 1395–1397 (2017).
38. Onoda, Y. et al. Physiological and structural tradeoffs underlying the leaf economics spectrum. *New Phytol.* **214**, 1447–1463 (2017).
39. Chavana-Bryant, C. et al. Leaf aging of Amazonian canopy trees as revealed by spectral and physiochemical measurements. *New Phytol.* **214**, 1049–1063 (2017).
40. Huang, M. et al. Velocity of change in vegetation productivity over northern high latitudes. *Nat. Ecol. Evol.* **1**, 1649–1654 (2017).
41. Malhi, Y. & Wright, J. Spatial patterns and recent trends in the climate of tropical rainforest regions. *Phil. Trans. R. Soc. B* **359**, 311–329 (2004).
42. Duffy, P. B., Brando, P., Asner, G. P. & Field, C. B. Projections of future meteorological drought and wet periods in the Amazon. *Proc. Natl Acad. Sci. USA* **112**, 13172–13177 (2015).
43. Thomas, S. C. Increased leaf reflectance in tropical trees under elevated CO₂. *Glob. Chang. Biol.* **11**, 197–202 (2005).
44. Michaletz, S. T. et al. The energetic and carbon economic origins of leaf thermoregulation. *Nat. Plants* **2**, 16129 (2016).
45. Helliker, B. R. & Richter, S. L. Subtropical to boreal convergence of tree-leaf temperatures. *Nature* **454**, 511–514 (2008).
46. Keenan, T. F. et al. Increase in forest water-use efficiency as atmospheric carbon dioxide concentrations rise. *Nature* **499**, 324–327 (2013).
47. van der Sleen, P. et al. No growth stimulation of tropical trees by 150 years of CO₂ fertilization but water-use efficiency increased. *Nat. Geosci.* **8**, 24–28 (2015).
48. Doughty, C. E. & Goulden, M. L. Are tropical forests near a high temperature threshold? *J. Geophys. Res. Biogeosci.* **113**, G00B07 (2008).
49. Mau, A. C., Reed, S. C., Wood, T. E. & Cavaleri, M. A. Temperate and tropical forest canopies are already functioning beyond their thermal thresholds for photosynthesis. *Forests* **9**, 47 (2018).
50. Zhu, P. et al. Elevated atmospheric CO₂ negatively impacts photosynthesis through radiative forcing and physiology-mediated climate feedback. *Geophys. Res. Lett.* **44**, 1956–1963 (2017).
51. *GEMTraits: A Database and R Package for Accessing and Analyzing Plant Functional Traits from the Global Ecosystems Monitoring Network* version 1 (Univ. Oxford, 2017); <https://ora.ox.ac.uk/objects/uuid:4101e249-3cf5-443f-9c29-9204604c667b>
52. Malhi, Y. et al. The variation of productivity and its allocation along a tropical elevation gradient: a whole carbon budget perspective. *New Phytol.* **214**, 1019–1032 (2017).
53. Hurrell, J. W., Hack, J. J., Shea, D., Caron, J. M. & Rosinski, J. A new sea surface temperature and sea ice boundary dataset for the community atmosphere model. *J. Clim.* **21**, 5145–5153 (2008).
54. IPCC *Climate Change 2014: Synthesis Report* (eds Core Writing Team, Pachauri, R. K. & Meyer L. A.) (IPCC, 2014).
55. Olivier, J. G. J., Janssens-Maenhout, G., Muntean, M. & Peters, J. A. H. W. *Trends in Global CO₂ Emissions: 2016 Report* (PBL Netherlands Environmental Assessment Agency and European Commission, Joint Research Centre, 2016); http://edgar.jrc.ec.europa.eu/news_docs/jrc-2016-trends-in-global-co2-emissions-2016-report-103425.pdf

Acknowledgements

This work is a product of the GEM network (gem.tropicalforests.ox.ac.uk), ABERG (andesresearch.org), the Amazon Forest Inventory Network (www.rainfor.org) and the Carnegie Spectranomics Project (spectranomics.carnegiescience.edu) research consortia. The field campaign was funded by a grant to Y.M. from the UK Natural Environment Research Council (NERC) (grant no. NE/I023418/1), with additional support from European Research Council advanced investigator grants GEM-TRAITS (no. 321131) and T-FORCES (no. 291585), and a John D. and Catherine T. MacArthur Foundation grant to G.P.A. We thank the Servicio Nacional de Áreas Naturales Protegidas por el Estado and the personnel of the Manu and Tambopata National Parks for logistical assistance and permission to work in the protected areas. We also thank the Explorers' Inn and the Pontifical Catholic University of Peru, as well as Asociación para la Conservación de la Cuenca Amazónica. We thank E. Cosio (Pontifical Catholic University of Peru) for his assistance with research permissions and sample analysis and storage. Taxonomic work at the Carnegie Institution was helped by R. Tupayachi, F. Sinca and N. Jaramillo. B.B. was supported by a United States National Science Foundation (NSF) graduate research fellowship and doctoral dissertation improvement grant (no. DEB-1209287), as well as an NERC independent research fellowship (grant no. NE/M019160/1). G.P.A. and the Spectranomics team were supported by the endowment of the Carnegie Institution for Science and a grant from the NSF (no. DEB-1146206). S.D. was partially supported by a Visiting Professorship grant from the Leverhulme Trust, UK. Y.M. was also supported by the Jackson Foundation. G.R.G. was supported by funding from the European Community's Seventh Framework Program (FP7/2007–2013) under grant agreement no. 290605 (COFUND: PSI-FELLOW). C.E.D. received funding from the John Fell Fund, Google and a NASA grant (no. 80NSSC17K0749). Climate simulations were run on Monsoon, Northern Arizona University's supercomputer.

Author contributions

C.E.D. wrote the paper with contributions from G.P.A., B.B., G.R.G. and R.E.M. P.E.S.-A. and C.E.D. collected the spectral data. P.E.S.-A., A.S., L.P.B., G.R.G., B.B., N.S., B.J.E., R.E.M., G.P.A., S.D. and Y.M. provided data or support. C.E.D. analysed the data and ran the climate and leaf reflectance simulations.

Competing interests

The authors declare no competing interests.

Additional information

Supplementary information is available for this paper at <https://doi.org/10.1038/s41559-018-0716-y>.

Reprints and permissions information is available at www.nature.com/reprints.

Correspondence and requests for materials should be addressed to C.E.D.

Publisher's note: Springer Nature remains neutral with regard to jurisdictional claims in published maps and institutional affiliations.

© The Author(s), under exclusive licence to Springer Nature Limited 2018

Reporting Summary

Nature Research wishes to improve the reproducibility of the work that we publish. This form provides structure for consistency and transparency in reporting. For further information on Nature Research policies, see [Authors & Referees](#) and the [Editorial Policy Checklist](#).

Statistical parameters

When statistical analyses are reported, confirm that the following items are present in the relevant location (e.g. figure legend, table legend, main text, or Methods section).

n/a | Confirmed

- The exact sample size (n) for each experimental group/condition, given as a discrete number and unit of measurement
- An indication of whether measurements were taken from distinct samples or whether the same sample was measured repeatedly
- The statistical test(s) used AND whether they are one- or two-sided
Only common tests should be described solely by name; describe more complex techniques in the Methods section.
- A description of all covariates tested
- A description of any assumptions or corrections, such as tests of normality and adjustment for multiple comparisons
- A full description of the statistics including central tendency (e.g. means) or other basic estimates (e.g. regression coefficient) AND variation (e.g. standard deviation) or associated estimates of uncertainty (e.g. confidence intervals)
- For null hypothesis testing, the test statistic (e.g. F , t , r) with confidence intervals, effect sizes, degrees of freedom and P value noted
Give P values as exact values whenever suitable.
- For Bayesian analysis, information on the choice of priors and Markov chain Monte Carlo settings
- For hierarchical and complex designs, identification of the appropriate level for tests and full reporting of outcomes
- Estimates of effect sizes (e.g. Cohen's d , Pearson's r), indicating how they were calculated
- Clearly defined error bars
State explicitly what error bars represent (e.g. SD, SE, CI)

Our web collection on [statistics for biologists](#) may be useful.

Software and code

Policy information about [availability of computer code](#)

Data collection

- We ran simulations using NCAR's Community Atmosphere Model (CAM 4.0; <http://www.cesm.ucar.edu/models/atm-cam/>)52, coupled with the Community Land Model (CLM 4.0; <http://www.cgd.ucar.edu/tss/clm/>) (compset F_2000_CN) with prescribed surface ocean temperatures53, a river transport model (RTM), and the Los Alamos sea ice model (CICE). Simulations were run at a 20 min time step with a resolution of 2° by 2.5° at the equator for 100 years. We ran the model with no dynamic vegetation response and atmospheric CO2 was held constant at 367 ppm for one set of runs and 700ppm for the other set.

Data analysis

We averaged the final 50 y of the following variables (collected monthly) from CLM 4.0: surface albedo (W m⁻²), latent heat flux (W m⁻²), sensible heat flux (W m⁻²), vegetation temperature (K), photosynthesis (μmol m⁻² sec⁻¹), and rainfall (mm sec⁻¹), and cloud cover (%) from CAM 4.0.

For manuscripts utilizing custom algorithms or software that are central to the research but not yet described in published literature, software must be made available to editors/reviewers upon request. We strongly encourage code deposition in a community repository (e.g. GitHub). See the Nature Research [guidelines for submitting code & software](#) for further information.

Data

Policy information about [availability of data](#)

All manuscripts must include a [data availability statement](#). This statement should provide the following information, where applicable:

- Accession codes, unique identifiers, or web links for publicly available datasets
- A list of figures that have associated raw data
- A description of any restrictions on data availability

Data Availability - All data in this paper can be found in a data repository with the following DOI:<https://ora.ox.ac.uk/objects/uuid:4101e249-3cf5-443f-9c29-9204604c667b>

Field-specific reporting

Please select the best fit for your research. If you are not sure, read the appropriate sections before making your selection.

Life sciences Behavioural & social sciences Ecological, evolutionary & environmental sciences

For a reference copy of the document with all sections, see [nature.com/authors/policies/ReportingSummary-flat.pdf](https://www.nature.com/authors/policies/ReportingSummary-flat.pdf)

Ecological, evolutionary & environmental sciences study design

All studies must disclose on these points even when the disclosure is negative.

Study description

We measured leaf traits and albedo during the CHAMBASA (CHallenging Attempt to Measure Biotic Attributes along the Slopes of the Andes) campaign from April – November 2013 along an elevation transect (from 3500 to 220 m asl) (Table S1) in the Peruvian Amazon⁵¹. The plots are part of a long-term research effort coordinated by the Andes Biodiversity Ecosystems Research Group (ABERG, <http://www.andesconservation.org>) and are part of the ForestPlots (<https://www.forestplots.net/>) and Global Ecosystems Monitoring Network (<http://gem.tropicalforests.ox.ac.uk/projects/aberg>). Plots were established between 2003 and 2013 in areas with minimal evidence of human disturbance. Within each plot, all stems ≥ 10 cm diameter at breast height are tagged and identified to species level. There is a negative linear relationship in the gradient between mean annual temperature (MAT) and elevation, with MAT of 24.4°C in the warmest lowland Amazonian site and 9.0°C at the Amazonian treeline in the Andes. Mean annual precipitation varies from 1560 to 5302 mm yr⁻¹ along the elevation gradient. Soils at elevations > 600 m asl are comprised of relatively high-fertility Inceptisols and Entisols. Soils at elevations < 600 m asl vary among Ultisols on low-fertility terra firme clay substrates and Inceptisols on inactive high-fertility floodplains. Plot characteristics are shown in Table S1.

Research sample

Leaf collections sampling strategy – In each 1 ha plot (N=10 plots), we sampled the most abundant species as determined through basal area weighting (enough species to account for 80% of the plot's basal area, although in the diverse lowland plots only 60-70% of plot basal area were sampled). For each species, we sampled the five (three in the lowlands) largest trees (based on diameter at breast height (DBH)) and tree climbers with extended tree pruners removed one fully sunlit and one shaded branch. These branches were quickly recut underwater to restore hydraulic conductivity. On each of these branches, we measured five randomly chosen leaves for photosynthesis and leaf spectral properties (generally measured within 1 hour of being cut). Leaf mass per unit area (LMA) for these leaves was measured on the same day.

Leaf spectroscopy - Hemispherical reflectance was measured on the top and bottom surface of five randomly selected leaves. The spectral measurements were taken at, or close to, the mid-point between the main vein and the leaf edge, and approximately halfway from the petiole to the leaf tip. Care was taken to avoid large primary or secondary veins, while allowing for smaller veins to be incorporated in the measurement. The spectra were collected with an ASD Fieldspec Handheld 2 with fibre optic cable contact probe that has its own calibrated light source and a leaf clip (Analytical Spectral Devices High Intensity Contact Probe and Leaf Clip, Boulder, Colorado, USA). The spectrometer records 750 bands spanning the 325–1075 nm wavelength region. Measurements were collected with 136-ms integration time per spectrum. We optimized the spectrometer after every branch. We calibrated the spectrometer on every leaf for dark current, stray light, and white referenced the measurement to a calibration panel (Spectralon, Lasphere, Durham, New Hampshire, USA). We averaged 25 individual spectrum per leaf to improve the signal-to-noise ratio of the data. We compared leaf albedo to LMA using a linear regression model.

Sampling strategy

In each 1 ha plot (N=10 plots), we sampled the most abundant species as determined through basal area weighting (enough species to account for 80% of the plot's basal area, although in the diverse lowland plots only 60-70% of plot basal area were sampled). For each species, we sampled the five (three in the lowlands) largest trees (based on diameter at breast height (DBH)) and tree climbers with extended tree pruners removed one fully sunlit and one shaded branch.

Data collection

In each 1 ha plot (N=10 plots), we sampled the most abundant species as determined through basal area weighting (enough species to account for 80% of the plot's basal area, although in the diverse lowland plots only 60-70% of plot basal area were sampled). For each species, we sampled the five (three in the lowlands) largest trees (based on diameter at breast height (DBH)) and tree climbers with extended tree pruners removed one fully sunlit and one shaded branch.

Timing and spatial scale

April – November 2013 along an elevation transect (from 3500 to 220 m asl) Table S1) in the Peruvian Amazon

Data exclusions

Data were excluded if > 3 sd +- mean.

Reproducibility

Randomization

Blinding

Did the study involve field work? Yes No

Field work, collection and transport

Field conditions

Location

Access and import/export

Disturbance

Reporting for specific materials, systems and methods

Materials & experimental systems

- n/a Involved in the study
- Unique biological materials
- Antibodies
- Eukaryotic cell lines
- Palaeontology
- Animals and other organisms
- Human research participants

Methods

- n/a Involved in the study
- ChIP-seq
- Flow cytometry
- MRI-based neuroimaging